Front. Earth Sci. 2018, 12(1): 148–159
https://doi.org/10.1007/s11707-016-0617-y

RESEARCH ARTICLE

The pore structure and fractal characteristics of shales with low thermal maturity from the Yuqia Coalfield, northern Qaidam Basin, northwestern China

Haihai HOU[1], Longyi SHAO (✉)[1], Yonghong LI[2], Zhen LI[1], Wenlong ZHANG[2], Huaijun WEN[2]

1 School of Geoscience and Surveying Engineering, China University of Mining and Technology, Beijing 100083, China
2 No.105 Exploration Team, Qinghai Bureau of Coal Geological Exploration, Xining 810007, China

Abstract The continental shales from the Middle Jurassic Shimengou Formation of the northern Qaidam Basin, northwestern China, have been investigated in recent years because of their shale gas potential. In this study, a total of twenty-two shale samples were collected from the YQ-1 borehole in the Yuqia Coalfield, northern Qaidam Basin. The total organic carbon (TOC) contents, pore structure parameters, and fractal characteristics of the samples were investigated using TOC analysis, low-temperature nitrogen adsorption experiments, and fractal analysis. The results show that the average pore size of the Shimengou shales varied from 8.149 nm to 20.635 nm with a mean value of 10.74 nm, which is considered mesopore-sized. The pores of the shales are mainly inkbottle- and slit-shaped. The sedimentary environment plays an essential role in controlling the TOC contents of the low maturity shales, with the TOC values of shales from deep to semi-deep lake facies (mean: 5.23%) being notably higher than those of the shore-shallow lake facies (mean: 0.65%). The fractal dimensions range from 2.4639 to 2.6857 with a mean of 2.6122, higher than those of marine shales, which indicates that the pore surface was rougher and the pore structure more complex in these continental shales. The fractal dimensions increase with increasing total pore volume and total specific surface area, and with decreasing average pore size. With increasing TOC contents in shales, the fractal dimensions increase first and then decrease, with the highest value occurring at 2% of TOC content, which is in accordance with the trends between the TOC and both total specific surface area and total pore volume. The pore structure complexity and pore surface roughness of these low-maturity shales would be controlled by the combined effects of both sedimentary environments and the TOC contents.

Keywords shale gas, pore structure, fractal dimension, Yuqia Coalfield, Jurassic, northern Qaidam Basin

1 Introduction

It is well known that shale gas is a clean and efficient unconventional natural gas. Ever since a breakthrough development in shale gas was achieved in the United States, many countries and regions with abundant shale gas resources have performed their own shale gas exploration and development (Zhang et al., 2004; Fildani et al., 2005; Montgomery et al., 2005; Bowker, 2007; Bernard et al., 2012; Wang et al.,. 2014). In 2011, the study "Shale gas resource evaluation and selection of favorable areas in China" was conducted by the Ministry of Land and Resources, and the total shale gas geological resources and recoverable resources in the continental basins of China were evaluated to be 134.42×10^{12} m^3 and 25.08×10^{12} m^3, respectively (Zhang et al., 2012). The shale gas potential in the Qaidam Basin was also investigated, and the shale gas geological resources and recoverable resources in this basin were determined to be 2.72×10^{12} m^3 and 0.56×10^{12} m^3 respectively, which demonstrate a promising future for shale gas exploration and development in this region. There are several sets of shales in the northern Qaidam Basin, including the Upper Carboniferous Hurleg Formation and the Middle Jurassic Shimengou and Damengou Formations. Several studies on the shale resources and pore structures in this region have been performed (Shao et al., 2014, 2016; Li et al., 2015; Liu et al., 2015a).

The pore characteristics of shales are always hard to describe quantitatively because shale reservoirs are

Received March 15, 2016; accepted September 18, 2016

E-mail: shaol@cumtb.edu.cn

complex and heterogeneous like coals. Fractal theory has become a useful tool for the description and quantitative evaluation of the pore structure (Pfeifer and Avnir, 1983; Pyun and Rhee, 2004). It is generally acknowledged that the value of the fractal dimension ranges from 2 to 3, with the value 2 representing a very smooth pore surface and homogeneous pore structure, and the value 3 signifying a very rough pore surface and complex pore structure (Xie, 1996; Pyun and Rhee, 2004). Based on experimental studies of low-temperature nitrogen adsorption, different methods for calculating the fractal dimension have been proposed, including the Frenkel-Halsey-Hill (FHH) model, the Brunauer-Emmtt-Teller (BET) model and the thermodynamic model (Nakagawa et al., 2000; Gauden et al., 2001; Li et al., 2016). Among these models, the fractal FHH method has proven to be useful and effective for porous materials (Xiao et al., 2013; Yang et al., 2014; Liang et al., 2015; Liu et al., 2015b; Tang et al., 2015). Yang et al. (2014), Liang et al. (2015) and Li et al. (2016) analyzed the fractal characteristics of marine shales with high maturity from the Upper Ordovician Wufeng Formation and the Lower Cambrian Niutitang and Qiongzhusi Formations of the Sichuan Basin, and discussed the relationships between the fractal dimension and both permeability and adsorption capacity. Liu et al. (2015b) investigated the pore structure and fractal characteristics of organic-rich continental shales with moderate-to-high maturity from the Upper Triassic Yanchang Formation in the Ordos Basin. Wang et al. (2015) analyzed the correlations between the pore structure parameters and the fractal dimensions of lacustrine shales from the Upper Cretaceous Qingshankou Formation in the Songliao Basin. Although a number of related topics have been discussed, few reports have been made about the fractal characteristics of the continental organic-rich shales with low thermal maturity in northwestern China.

For this study, the fractal dimensions of shales of the Yuqia Coalfield in the northern Qaidam Basin were calculated based on low-temperature nitrogen adsorption data with the fractal FHH method, and the relationships between total organic carbon (TOC) contents, pore structure parameters, and the fractal dimensions were investigated in detail. It is hoped that these data and results can contribute to a deeper understanding of the pore structure system of continental shales with low thermal maturity.

2 Geological setting

The Yuqia Coalfield is located in the central belt of the northern Qaidam Basin, northwestern China (Fig. 1). The Middle Jurassic succession in this basin is up to 1 km in thickness and includes the Dameigou Formation and the overlying Shimengou Formation. The Shimengou Formation, composed of continental coarse to fine-grained

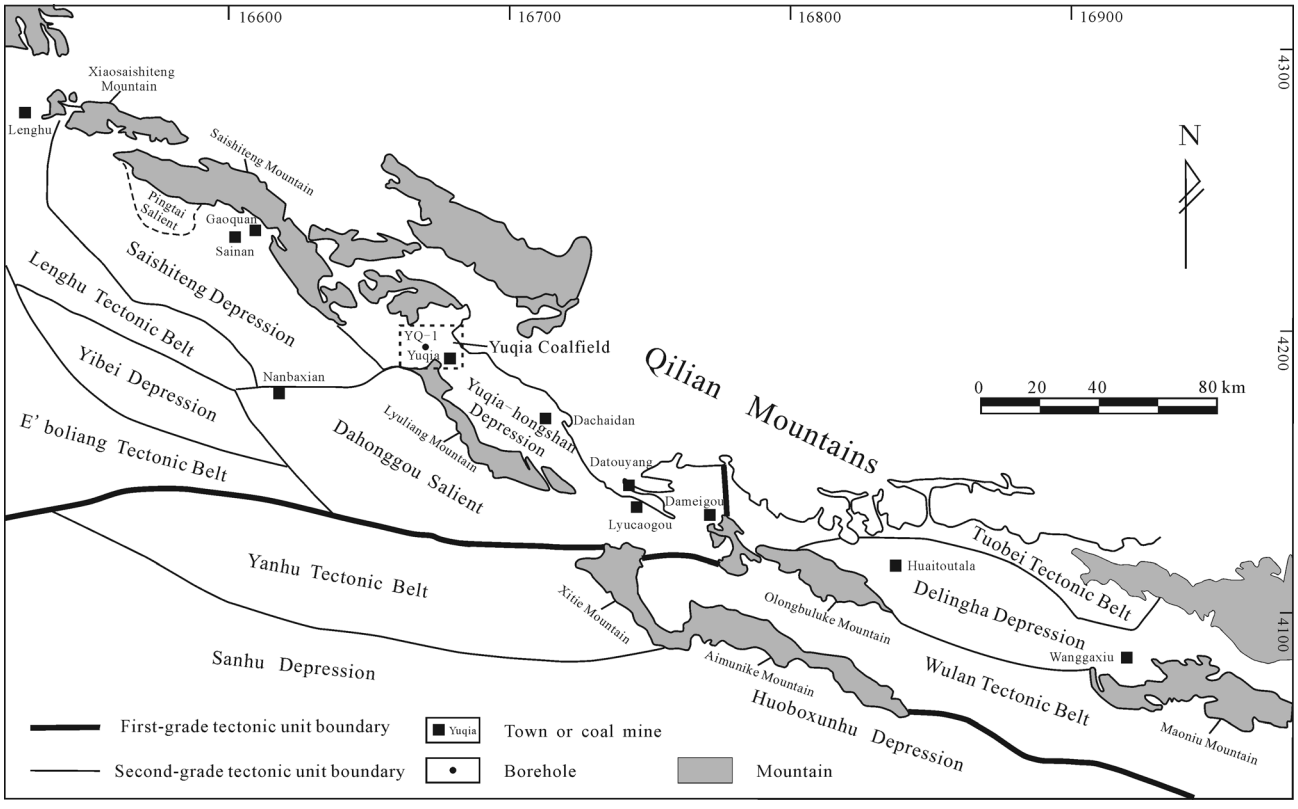

Fig. 1 The location of the studied site and tectonic position of the Yuqia Coalfield, northern Qaidam Basin.

siliciclastic rocks, mudstone/shale, oil shale, and thin coal seams, is the main horizon for shale gas exploration (Fig. 2). This formation has been subdivided into two members: the Lower Member and the Upper Member. The Lower Member includes over 10 m thick fine-grained sandstones and siltstones at its base, thick gray sandstone-mudstone intercalations in the middle section, and gray black mudstone in the upper part, whereas the Upper Member contains white medium- to coarse-grained sandstones at its base, gray fine sandstone and siltstone in the middle, and thick, black mudstone and oil shale in the upper part. Among these units, the shale and mudstones of the upper part of the Upper Member and middle-to-upper part of the Lower Member are the main shale horizons.

According to a previous study (Li et al., 2014), the Shimengou Formation was deposited in the lower delta plain and lacustrine sedimentary environments. The middle-to-upper section of the Lower Member was deposited in a shoreline-shallow lake setting, whereas the upper part of the Upper Member formed in a deep to semi-deep lake environment (Fig. 2).

3 Samples and experimental methods

A total of 22 shale samples were collected from the YQ-1 borehole in the Yuqia Coalfield, including 13 samples from

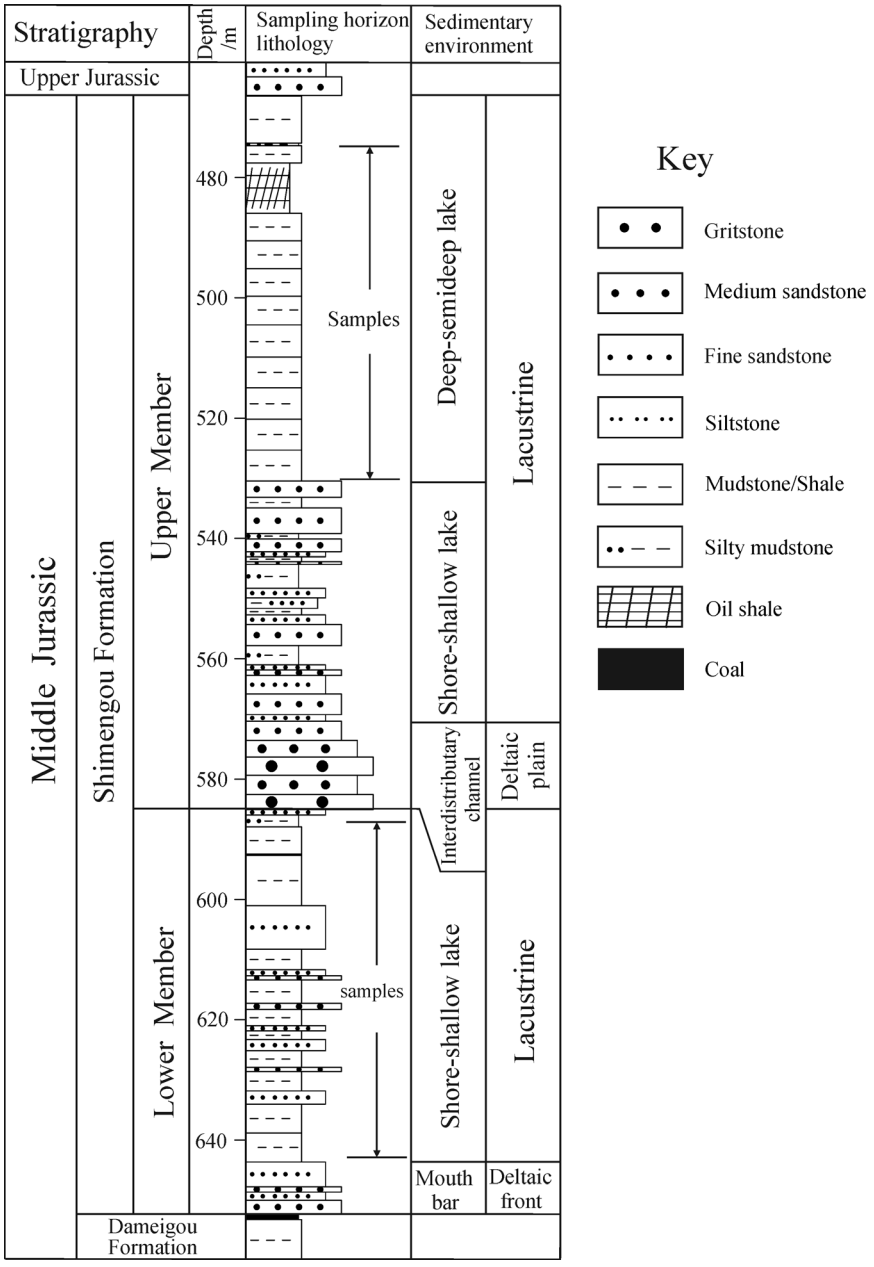

Fig. 2 The lithology and sedimentary environments of the Shimengou Formation, as well as the sampled positions of the YQ-1 borehole.

the Upper Member and 9 samples from the Lower Member (Fig. 2). All the samples were analyzed for TOC content, vitrinite reflectance, and low-temperature nitrogen adsorption.

The TOC contents were determined by the LECO CS230 carbon/sulfur analyzer. The samples, treated by hydrochloric acid solution, were crushed to grains less than 100 mesh size, then 0.1–1 g samples were pyrolyzed up to 540°C for 2 hours following the Chinese National standards GB/T 19145-2003 and GB/T 18602-2001.

Vitrinite reflectance was measured with oil immersion reflected light optics using a Leitz MPV-3 photometer microscope in accordance with the Chinese National Standards GB/T 6948-1998. For each sample, approximately 40 different vitrinite observation points were selected for measurement, and the averaged data of these measurements were used.

The low-temperature nitrogen adsorption experiment is generally used to test specific surface area, pore volume, and pore structure distribution of shale samples following the China Petroleum Industry Standard SY/T6154-1995. We conducted this experiment with a Micromeritic TriStar II 3020 surface area and pore size analyzer. All the samples were sieved to a size range of 0.28 mm to 0.42 mm, each weighing up 10 g for the experiment. For each sample, the nitrogen adsorption-desorption isotherm can be derived under relative pressure ranging from 0.01 to 0.99 at 77 K. Based on the adsorption data of all samples, the total specific surface area was calculated using the BET equation under the relative pressure ranging from 0.05–0.35 (Brunauer et al., 1938; Gregg and Sing, 1982), and pore size distribution (PSD) was determined with the BJH (Barrett-Joyner-Halenda) method (Barret et al., 1951). The average pore size can be calculated based on the relationship between total specific surface area and total pore volume combined with a pore model. According to the BJH pore volume and cylindrical pore model, the incremental pore volume and incremental surface area of some relative pressure range can be calculated with the following equations as follows (Micromeritics Instrument Corporation, 2012):

$$V_{\mathrm{PI}} = 10^{-16}\eth(L_{\mathrm{PI}})\left[\frac{D_{\mathrm{avg_I}}}{2}\right]^2, \tag{1}$$

$$SA_{\mathrm{PI}} = 10^{-12}\eth(L_{\mathrm{PI}})(\mathrm{D}_{\mathrm{avg_I}}), \tag{2}$$

where, V_{PI} is the incremental pore volume ($\mathrm{cm^3\cdot g^{-1}}$); SA_{PI} is the incremental surface area ($\mathrm{m^2\cdot g^{-1}}$); L_{PI} is the incremental length of pores ($\mathrm{cm\cdot g^{-1}}$); and $D_{\mathrm{avg_I}}$ is the incremental average pore diameter (Å). Therefore, the volumes and surface areas in specified pore size ranges can be obtained. For this study, pores were subdivided into micropores (<5 nm), mesopores (5 nm to 50 nm), and macropores (>50 nm) (Luo et al., 2014; Shao et al., 2016). Therefore, the cumulative pore volume and cumulative surface area of pore size smaller than 5 nm represents the micropore volume and micropore specific area, respectively.

4 Results

4.1 The maturity and TOC of shales

From Table 1, we observe that R_{o} values of the shale samples are between 0.36% and 0.66% with an average value of 0.47%, and thus, fall into the low thermal maturity stage. TOC contents range from 0.27% to 9.35%, with an average of 3.36%, indicating that the Shimengou shales are rich in organic matter. Furthermore, the TOC contents generally decrease with increasing R_{o} values (Table 1), which suggests that the shales with higher R_{o} values and lower TOC contents have less adsorbed gas (Chalmers and Bustin, 2008).

4.2 The pore structure of shale samples based on the nitrogen adsorption-desorption isotherms

The nitrogen adsorption-desorption isotherms of typical shale samples in this study are shown in Fig. 3. According to the classification of the International Union of Pure and Applied Chemistry (IUPAC), the nitrogen adsorption-desorption isotherms of shale samples belong to type IV (Sing, 1982). Based on the shape of adsorption-desorption isotherms, the samples typically showed hysteresis loops, and two types were subdivided according to the morphology of the hysteresis loops: type A (e.g., YQ-1-8) and type B (e.g., YQ-1-19). For type A, when relative pressure is low, the adsorption branch is coincident with the desorption branch. However, when relative pressure increases, the adsorption and desorption branches separate, which leads to a distinct hysteresis loop. The hysteresis loop of type B does not show the plateau at the high relative pressure compared with type A. Therefore, the shale samples of type A are mainly characterized by inkbottle-shaped pores and the samples of type B by slit-shaped pores.

4.3 Specific surface area, pore volume, and average pore size

The specific surface area, pore volume, and average pore size of the Shimengou shales are shown in Table 1. The specific surface area ranges from 2.2662 $\mathrm{m^2\cdot g^{-1}}$ to 20.2712 $\mathrm{m^2\cdot g^{-1}}$, with a mean value of 11.55 $\mathrm{m^2\cdot g^{-1}}$, about 12 times more than that of a conventional sandstone reservoir (Donaldson et al., 1975). The total pore volume is found to be between 12.469 $\times 10^{-3}$ $\mathrm{cm^3\cdot g^{-1}}$ and 38.307 $\times 10^{-3}$ $\mathrm{cm^3\cdot g^{-1}}$, with an average of 27.57×10^{-3} $\mathrm{cm^3\cdot g^{-1}}$. The average pore size is in the range from 8.149 nm to 20.635 nm with a mean value of 10.74 nm, which is

Table 1 TOC contents, vitrinite reflectance, and pore parameters of the shale samples determined with the nitrogen adsorption experiment.

Sample No.	Depth/m	TOC/%	R_o/%	A_s/($m^2 \cdot g^{-1}$)	V_t/($10^{-3} cm^3 \cdot g^{-1}$)	S_a/nm	A_{mic}/($m^2 \cdot g^{-1}$)	V_{mic}/($10^{-3} cm^3 \cdot g^{-1}$)
YQ-1-1	475.5–476.5	8.43	–	3.0094	17.756	20.635	1.217	0.883
YQ-1-2	479.5–480.5	6.88	–	4.3426	21.978	17.559	2.167	1.526
YQ-1-3	483.5–484.5	2.98	0.64	2.2662	12.469	18.738	1.209	0.842
YQ-1-4	491.5–492.5	9.35	–	12.3751	31.527	11.284	6.337	4.840
YQ-1-5	495.5–496.5	5.92	0.44	12.5456	31.327	11.238	6.433	4.895
YQ-1-6	499.5–500.5	6.12	–	9.1602	25.06	11.09	5.145	4.046
YQ-1-7	503.5–504.5	3.75	0.39	17.7593	34.247	8.611	10.145	7.669
YQ-1-8	507.5–508.5	8.11	–	5.8828	19.086	11.66	3.301	2.521
YQ-1-9	511.5–512.5	3.23	0.37	12.7104	32.48	10.235	7.476	5.875
YQ-1-10	515.5–516.5	2.83	–	14.3149	35.006	9.901	8.493	6.700
YQ-1-11	519.5–520.5	1.81	0.40	18.3285	38.307	8.483	11.419	9.051
YQ-1-12	523.5–524.5	4.76	–	12.9194	30.924	8.946	7.824	6.058
YQ-1-13	527.5–528.5	3.83	0.36	14.0817	32.749	8.662	8.842	6.833
YQ-1-14	584.5–585.5	0.32	–	8.3136	18.621	8.993	5.255	4.140
YQ-1-15	588.5–589.5	0.64	0.66	12.9595	25.971	8.61	7.597	5.760
YQ-1-16	592.5–593.5	0.55	–	13.9949	29.267	8.59	8.628	6.848
YQ-1-17	615.5–616.5	0.41	–	12.7884	25.421	8.149	7.954	6.341
YQ-1-18	620.5–621.5	1.24	0.65	20.2712	36.244	7.794	12.138	9.136
YQ-1-19	624.5–625.5	0.27	–	11.7147	27.412	9.197	7.211	5.630
YQ-1-20	628.5–629.5	0.44	–	12.3261	27.758	9.029	7.405	5.854
YQ-1-21	635.5–636.5	1.12	0.48	13.0032	30.258	9.078	7.969	6.216
YQ-1-22	641.5–642.5	0.86	–	9.1144	22.727	9.705	5.483	4.260

–, no data. R_o, vitrinite average reflectance; A_s, total specific surface area; V_t, total pore volume; S_a, average pore size; A_{mic}, the specific surface area of micropores; V_{mic}, the pore volume of micropores.

considered to be mesopore sized. Furthermore, the micropore surface area and micropore volume range from 1.209 $m^2 \cdot g^{-1}$ to 12.138 $m^2 \cdot g^{-1}$ (with an average of 6.802 $m^2 \cdot g^{-1}$) and from 0.842 $\times 10^{-3}$ $cm^3 \cdot g^{-1}$ to 9.136 $\times 10^{-3}$ $cm^3 \cdot g^{-1}$ (with an average of 5.269×10^{-3} $cm^3 \cdot g^{-1}$), respectively.

4.4 Fractal dimension from the nitrogen adsorption isotherms

According to the fractal FHH model, the equation for calculating fractal dimensions of shales can be described as follows (Pyun and Rhee, 2004; Yao et al., 2008):

$$\ln\left(\frac{V}{V_o}\right) = \text{constant} + A\left[\ln\left(\ln\left(\frac{P_o}{P}\right)\right)\right], \quad (3)$$

where V is the adsorbed gas volume at the equilibrium pressure P; V_o is the monolayer volume of adsorbed gas; P_o is the saturation gas pressure; and A is the slope between $\ln\left(\ln\left(\frac{P_o}{P}\right)\right)$ and $\ln\left(\frac{V}{V_o}\right)$.

The double logarithmic curves between the adsorption volume and the P_o/P of typical shale samples exhibit a straight line at the relative pressure stage (Fig. 4). Based on this method, the linear fitting coefficients of determination (R^2) for all samples can be obtained (Table 2), which are greater than 0.96, suggesting that these shale samples do have fractal characteristics. It is worth noting that there are two separate fractal characteristics under the different relative pressure ranges (Yao et al., 2008; Wang et al., 2015; Li et al., 2016), and for this study, a single fractal dimension for each sample would be appropriate due to the fitting degree of obtained double logarithmic curves (Yang et al., 2014; Liang et al., 2015). Furthermore, there are two formulas used to calculate the fractal dimensions using the linear slopes (A) (Qi et al., 2002; Pyun and Rhee, 2004; Rigby, 2005), that is '$D = 3 + A$' and '$D = 3 + 3A$', respectively. As shown in Table 2, the fractal dimensions calculated by the equation '$D = 3 + A$' are between 2 and 3, whereas most of the fractal dimensions calculated with the other equation '$D = 3 + 3A$' are less than 2, which stray from the definition of the fractal dimensions (Pfeifer and Avnir, 1983; Xie, 1996). Therefore, the fractal dimensions calculated with the expression of '$D = 3 + A$' were used for this study because of these more realistic values. Mean-

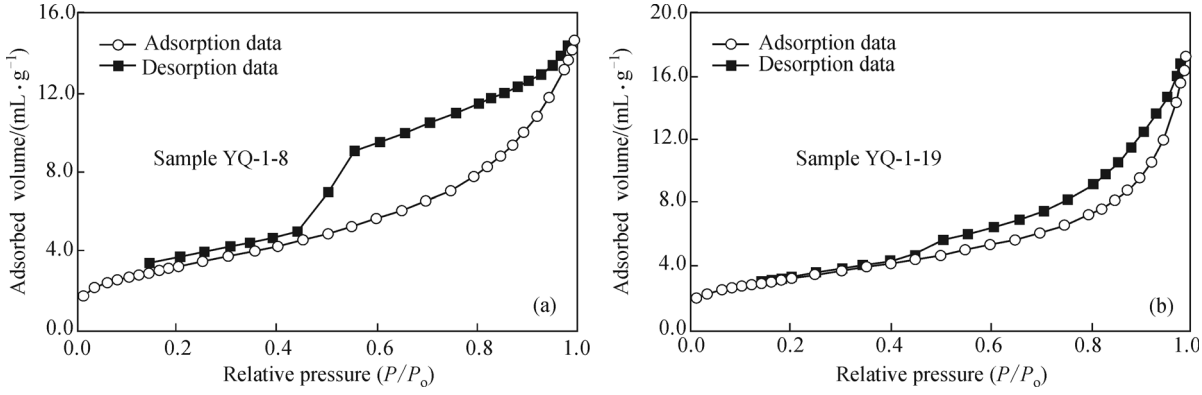

Fig. 3 The nitrogen adsorption-desorption curves of typical shale samples from the Shimengou Formation.

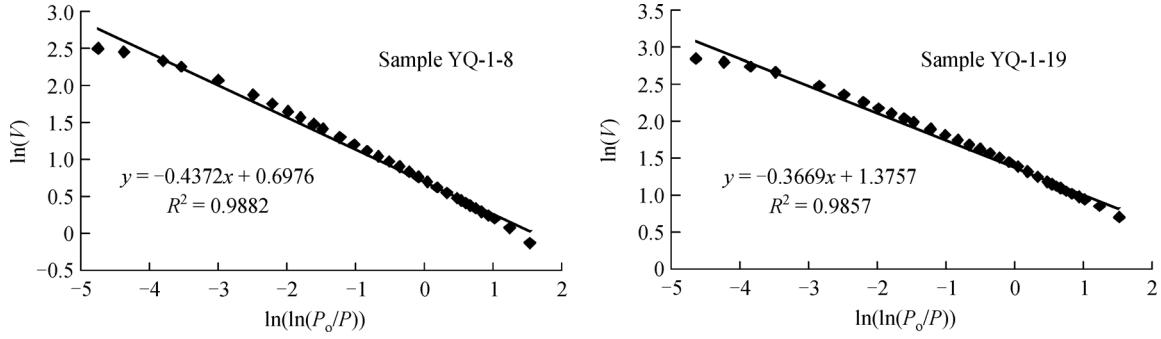

Fig. 4 Double logarithmic curves between adsorption volume and P_o/P for typical shale samples.

while, a higher fractal dimension is characterized by more complex pore structure and rougher pore surface. The fractal dimensions used here range from 2.4639 to 2.6857 with an average of 2.6122, which are higher than those of marine shales of the Upper Ordovician Wufeng Formation in southeastern China (Liang et al., 2015), indicating a relatively rough pore surface and complex pore structure for the Shimengou shales.

5 Discussion

5.1 Controls of sedimentary environments on TOC contents and fractal dimensions

As shown in Fig. 5, the TOC contents of the shales decrease markedly with increasing depth. The main factor controlling this relationship is actually the sedimentary environment. Specifically, the shale samples from the Upper Member of the Shimengou Formation were deposited in deep to semi-deep lake environments, whereas the Lower Member was deposited in shore-shallow lake environments (Fig. 2). As deep to semi-deep lake deposits are characterized by more stable hydrodynamic conditions and finer-grained deposits than those of shore-shallow lake deposits (Zhu, 2008; Li et al., 2014), the TOC contents of the shale samples from the Upper Member are higher than those from the Lower Member. Furthermore, the average value of the fractal dimension of the shales from the Upper Member is 2.59, whereas the average value for the Lower Member is 2.65 (Table 2). Therefore, the pore structure is more complex and the pore surface is rougher in the shale formed in the shore-shallow lake environments.

5.2 Relationships between the specific surface area, pore volume, and average pore size

The relationships between the specific surface area, pore volume, and the average pore size are shown in Fig. 6. There is a positive correlation between the total specific surface area and the total pore volume; the linear fitting coefficient (R^2) is 0.8497 (Fig. 6(a)). This positive relationship becomes more apparent between the specific surface area and the volume of the micropores ($R^2 = 0.9972$ in Fig. 6(b)). There are negative relationships between the average pore size and both the total specific surface area and the total pore volume, with the linear fitting coefficients (R^2) of 0.6719 and 0.4356, respectively (Figs. 6(c) and 6(d)). These relationships are in accordance with previous studies for the shales (Chalmers et al., 2012; Yang et al., 2014; Liu et al., 2015b; Li et al., 2016), and for

Table 2 Fractal dimensions of the shale samples of the Yuqia Coalfield calculated with the fractal FHH equation

Sample No.	A	$D = 3 + A$	$D = 3 + 3A$	R^2
YQ-1-1	−0.5361	2.4639	1.3917	0.9968
YQ-1-2	−0.5126	2.4874	1.4622	0.9975
YQ-1-3	−0.5291	2.4709	1.4127	0.9946
YQ-1-4	−0.3763	2.6237	1.8711	0.9971
YQ-1-5	−0.3685	2.6315	1.8945	0.9964
YQ-1-6	−0.3925	2.6075	1.8225	0.9960
YQ-1-7	−0.3361	2.6639	1.9917	0.9875
YQ-1-8	−0.4372	2.5628	1.6884	0.9880
YQ-1-9	−0.3802	2.6198	1.8594	0.9920
YQ-1-10	−0.3718	2.6282	1.8846	0.9915
YQ-1-11	−0.3444	2.6556	1.9668	0.9809
YQ-1-12	−0.3953	2.6047	1.8141	0.9784
YQ-1-13	−0.3758	2.6242	1.8726	0.9697
YQ-1-14	−0.3533	2.6467	1.9401	0.9842
YQ-1-15	−0.3401	2.6599	1.9797	0.9831
YQ-1-16	−0.3475	2.6525	1.9575	0.9859
YQ-1-17	−0.3387	2.6613	1.9839	0.9785
YQ-1-18	−0.3143	2.6857	2.0571	0.9680
YQ-1-19	−0.3669	2.6331	1.8993	0.9857
YQ-1-20	−0.3601	2.6399	1.9197	0.9831
YQ-1-21	−0.3683	2.6317	1.8951	0.9805
YQ-1-22	−0.3848	2.6152	1.8456	0.9903

A, the slope of the straight line; R^2, the linear fitting coefficient.

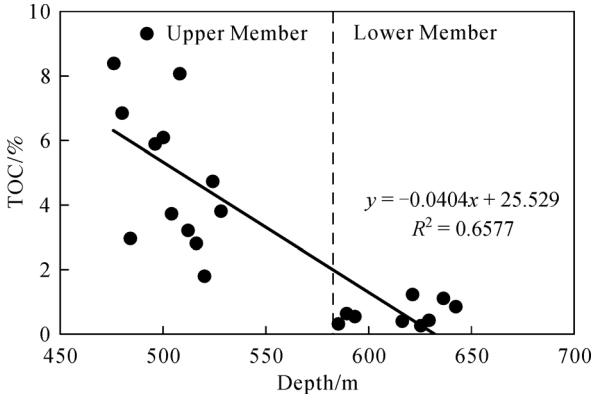

Fig. 5 Relationship between the TOC contents of shales and burial depth based on the sedimentary environments in the Yuqia Coalfield of the northern Qaidam Basin.

coals (Yao et al., 2008) from other areas. Furthermore, we can also observe that the average pore size is negatively correlated with both the micropore specific surface area and the micropore volume (Figs. 6(e) and 6(f)); their linear fitting coefficients (R^2) are 0.7182 and 0.7327, respectively. These relationships indicate that shales with smaller average pore sizes have higher micropore volumes and micropore specific surface areas, resulting in greater adsorption capacities (Yang et al., 2014).

5.3 Relationships between fractal dimensions and the specific surface areas, pore volumes, and average pore sizes

As shown in Fig. 7(a) and Fig. 7(b), the fractal dimension correlates positively with the total specific surface area and the total pore volume; the linear fit coefficients (R^2) are 0.7641 and 0.4952, respectively. These relationships indicate that the shales with higher fractal dimensions may have greater total specific surface areas and higher total pore volumes. In addition, we have found that the fractal dimension has a negative relationship with the average pore size of shale samples (Fig. 7(c)), suggesting that the shales with complex pore structure or rough pore surfaces (high fractal dimensions) have relatively small average pore sizes. Furthermore, significant positive relationships exist between the micropore specific surface areas, the micropore volumes, and the fractal dimensions (Fig. 7(d) and 7(e)), with linear fitting coefficients (R^2) of 0.7728 and 0.7806, respectively. Therefore, the micropore proportions of the Shimengou shales may have significant impacts on their fractal dimensions.

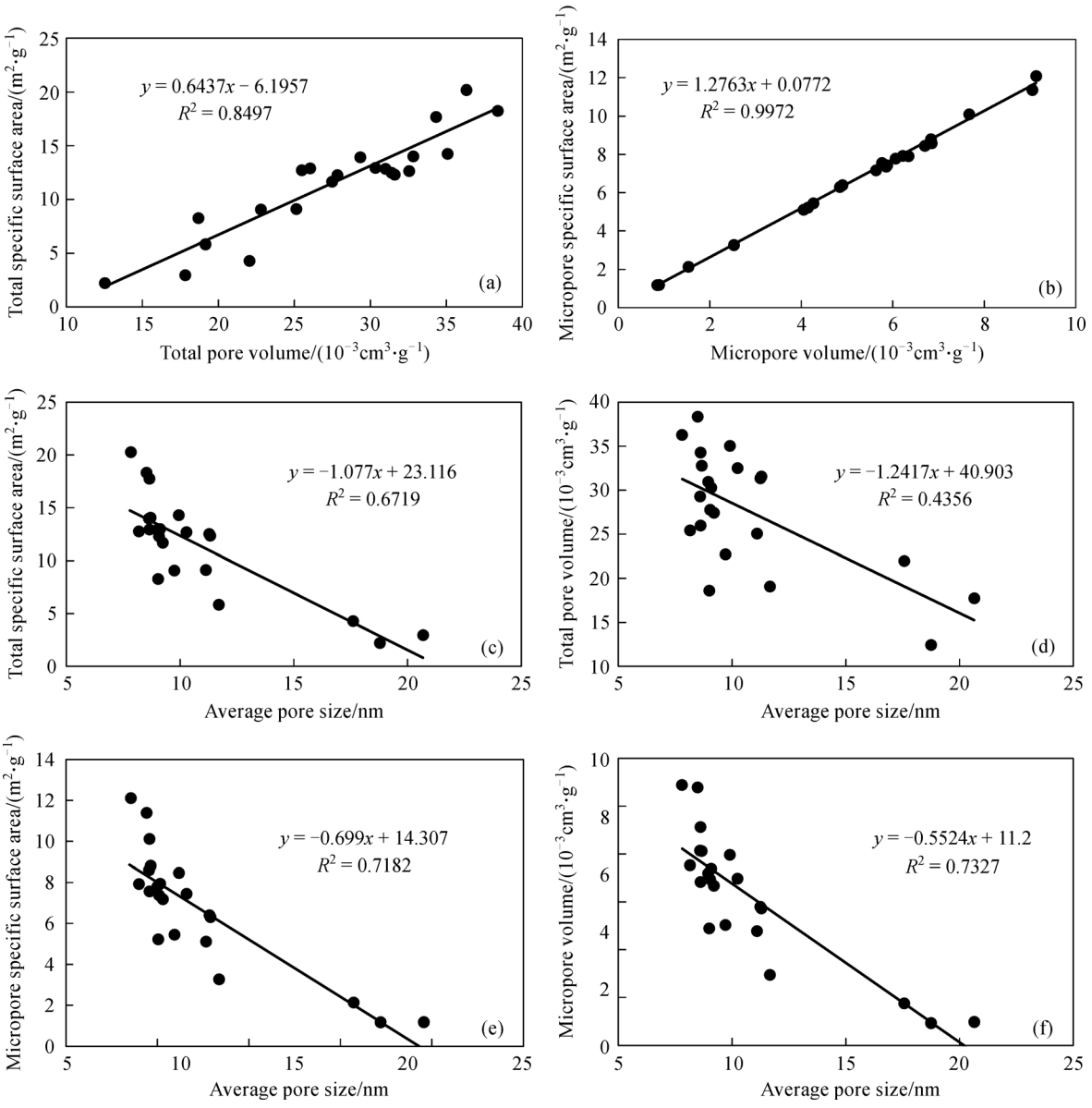

Fig. 6 Relationships between the specific surface areas, pore volumes, and average pore sizes of the shale samples from the Yuqia Coalfield, northern Qaidam Basin.

5.4 Relationship between the fractal dimensions and TOC contents of the shales

Previous studies have reported that the fractal dimensions of shales increase with increasing TOC content (Yang et al., 2014; Liu et al., 2015b; Li et al., 2016), or that the relationship between the two parameters follows a U-shaped curve (Wang et al., 2015). However, for the Shimengou shales in the northern Qaidam Basin, the fractal dimension first increases and then decreases with increasing TOC contents, and the highest fractal dimension value is reached at 2% of the TOC content (Fig. 8). During the low maturity stage of lacustrine shales, nano-scale pores (mainly in micropores) of organic matter are rare, and they are generally less in quantity than the mineral matrix pores (Dow, 1977; Loucks et al., 2012; Cao et al., 2015). Therefore, changes in organic micropores would play an important role in changing the pore structure and fractal characteristics (Figs. 7(d) and 7(e)). Meanwhile, supporting effects of shales developed in deep to semi-deep lake environment (relatively fine-grained deposits) are weaker than those deposited in shore-shallow lake settings (relatively coarse-grained deposits). When TOC content is less than 2%, micropore contents increase with increasing TOC (Wu et al., 2014), which can also be preserved under a stronger supporting force, thus, this positive effect results in higher total specific surface area and total pore volume (Figs. 9(a) and 9(b)). When the TOC

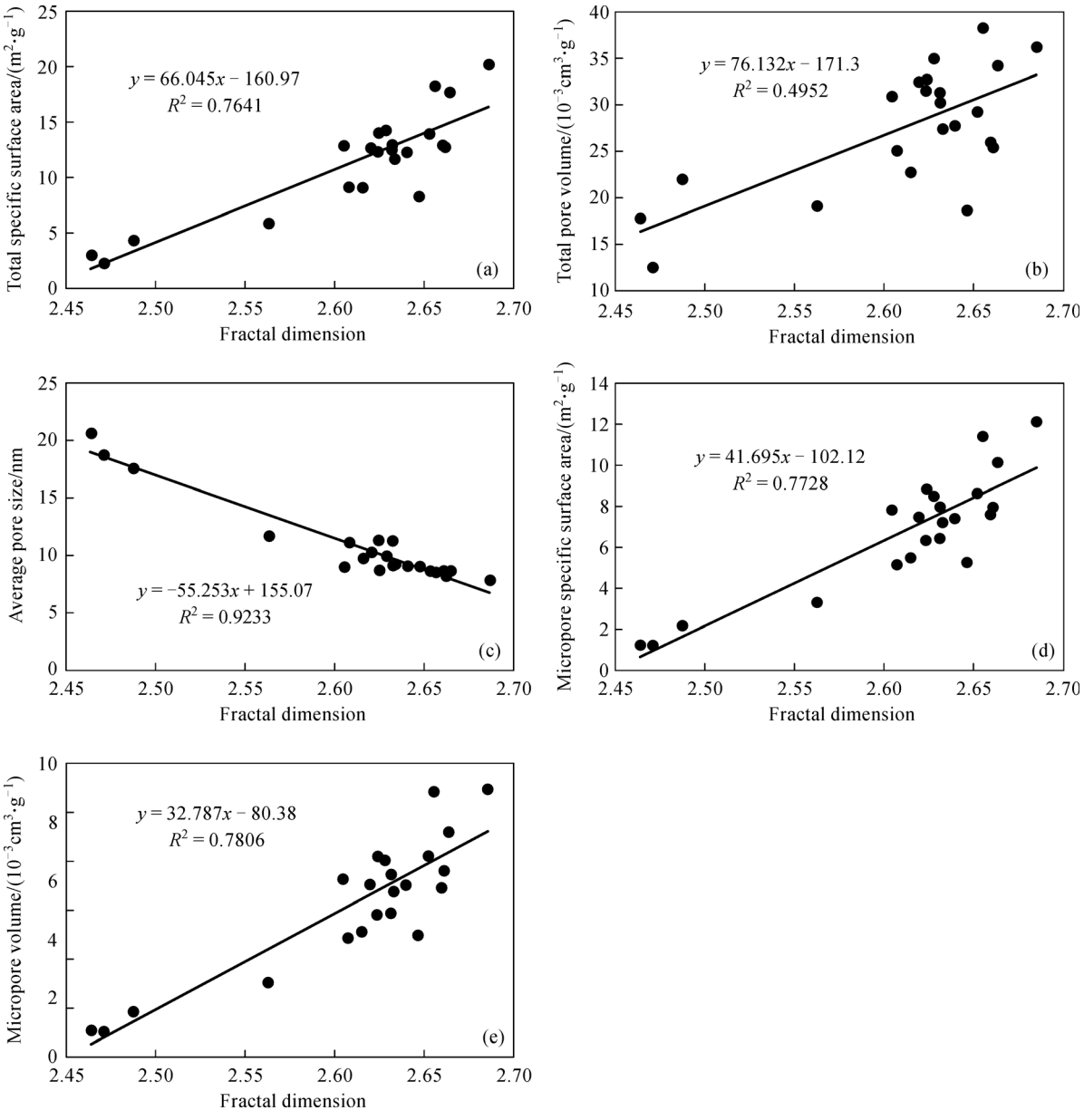

Fig. 7 Relationships between the specific surface areas, pore volumes, the average pore sizes, and the fractal dimensions of the shale samples from the Yuqia Coalfield, northern Qaidam Basin.

content is higher than 2%, the contents of the mineral matrix would decrease and some existing nano-scaled pores would be filled with excessive TOC under a relatively weaker supporting force, thus, the negative effects would become dominant and result in lower total specific surface area and total pore volume (Milliken et al., 2013). Therefore, in conjunction with the positive correlations of the fractal dimension with total specific surface area and total pore volume (Figs. 7(a) and 7(b)), the relationship between the fractal dimension and TOC content is characterized by an inverted U-shaped curve (Fig. 8). The combined effects of both sedimentary environment and TOC content thus control the pore structure complexity and pore surface roughness of low-maturity shales. Based on these relationships, we conclude that pore structure becomes more complex with increasing of TOC contents when the shales are from shore-shallow lake settings, whereas pore structure becomes more homogeneous with increasing TOC for shales deposited in deep to semi-deep lake environments.

6 Conclusions

(1) The average pore size of the Shimengou shales is within the range of 8.149−20.635 nm with a mean value of

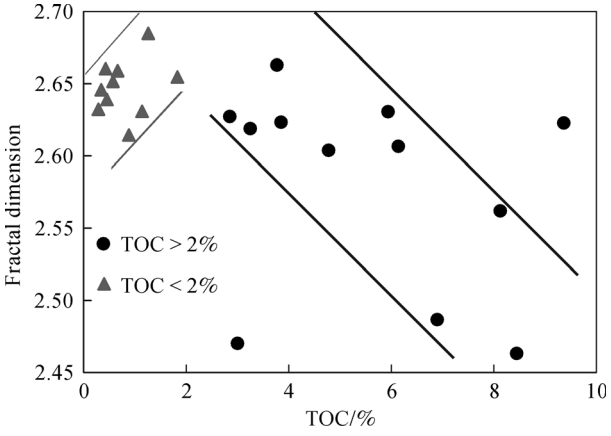

Fig. 8 Relationship between the fractal dimensions and TOC contents of the shales from the Shimengou Formation in the Yuqia Coalfield, northern Qaidam Basin.

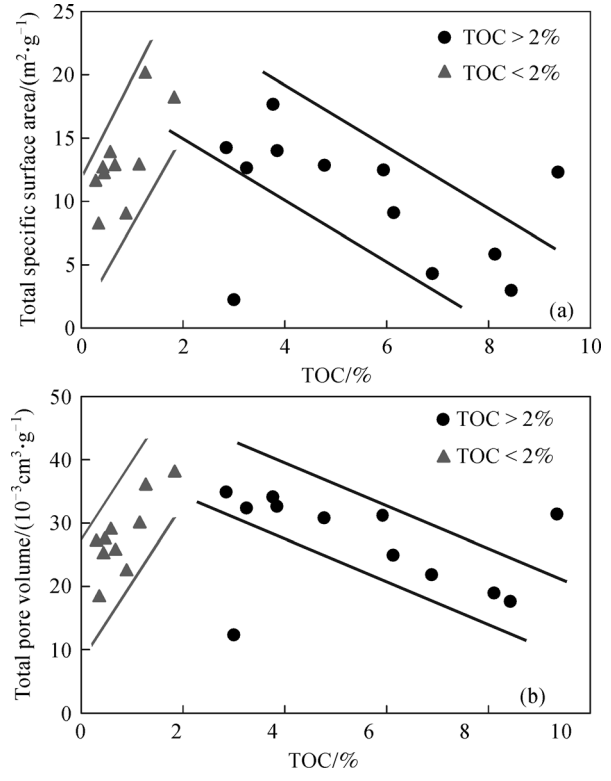

Fig. 9 Relationships of the TOC contents with the total specific surface areas and the total pore volumes of the shales from the Shimengou Formation in the Yuqia Coalfield, northern Qaidam Basin.

10.74 nm, which is considered as mesopore sized. These pores are mainly characterized by inkbottle and slit shapes.

(2) The TOC contents of the shales range from 0.27% to 9.35% with an average value of 3.36%, indicating that the Shimengou shales are rich in organic matter. The sedimentary environment plays a decisive role in determining the TOC contents, and the TOC contents of shales from deep-semideep lake environments are higher than those from shore-shallow lake settings.

(3) The fractal dimensions range from 2.4639 to 2.6857 with an average of 2.6122, higher than the typical values for marine shales, which indicates that the Shimengou shales have relatively rough pore surfaces and complex pore structures.

(4) The fractal dimensions increase with the increasing total pore volume and total specific surface area, and with decreasing average pore size. The fractal dimension first increases and then decreases with increasing TOC contents in the shales. The maximum fractal dimension value is reached at 2% of the TOC value, which is in accordance with the trends between the TOC contents and both the total specific surface areas and the total pore volumes. The combined effects of both sedimentary environment and TOC content thus control the complexity of the pore structure and roughness of the pore surface for low-maturity shales.

Acknowledgements This research was supported by the National Science and Technology Major Project (2016ZX05041004-003) and the China Geological Survey Scientific Research Project (12120114019501 and 1212011220794). The authors are grateful for the valuable comments from two anonymous reviewers.

References

Barrett E P, Joyner L G, Halenda P P (1951). The determination of pore volume and area distribution in porous substances. I. Computations from nitrogen isotherms. J Am Chem Soc, 73(1): 373–380

Bernard S, Horsfield B, Schulz H M, Wirth R, Schreiber A, Sherwood N (2012). Geochemical evolution of organic-rich shales with increasing maturity: a STXM and TEM study of the Posidonia Shale (Lower Toarcian, northern Germany). Mar Pet Geol, 31(1): 70–89

Bowker K A (2007). Barnett shale gas production, Fort Worth Basin: issues and discussion. AAPG Bull, 91(4): 523–533

Brunauer S, Emmett P H, Teller E (1938). Adsorption of gases in multimolecular layers. J Am Chem Soc, 60(2): 309–319

Cao T T, Song Z G, Luo H Y, Liu G X (2015). The differences of microscopic pore structure characteristics of coal, oil shale and shales and their storage mechanisms. Natural Gas Geoscience, 26(11): 2208–2218 (in Chinese)

Chalmers G R, Bustin R M (2008). Lower Cretaceous gas shales in northeastern British Columbia, Part I: geological controls on methane sorption capacity. Bull Can Pet Geol, 56(1): 1–21

Chalmers G R, Bustin R M, Power I M (2012). Characterization of gas shale pore systems by porosimetry, pycnometry, surface area, and field emission scanning electron microscopy/transmission electron microscopy image analyses: examples from the Barnett, Woodford, Haynesville, Marcellus, and Doig units. AAPG Bull, 96(6): 1099–1119

Donaldson E C, Kendall R F, Baker B A, Manning F S (1975). Surface-area measurement of geological matereials. Soc Pet Eng J, 15(02):

111–116

Dow W G (1977). Kerogen studies and geological interpretations. J Geochem Explor, 7(2): 79–99

Fildani A, Hanson A D, Chen Z Z, Moldowan J D, Graham S A, Arriola P R (2005). Geochemical characteristics of oil and source rocks and implication for petroleum system, Talara basin, northwest Peru. AAPG Bull, 89(11): 1519–1545

Gauden P A, Terzyk A P, Rychlicki G (2001). The new correlation between microporosity of strictly microporous activated carbons and fractal dimension on the basis of the Polanyi-Dubinin theory of adsorption. Carbon, 39(2): 267–278

Gregg S J, Sing K S W (1982). Adsorption, Surface Area and Porosity (2nd ed). London: Academic Press, 42–55

Li A, Ding W L, He J H, Dai P, Yin S, Xie F (2016). Investigation of pore structure and fractal characteristics of organic-rich shale reservoirs: a case study of Lower Cambrian Qiongzhusi Formation in Malong block of eastern Yunnan Province, South China. Mar Pet Geol, 70: 46–57

Li M, Shao L Y, Lu J, Spiro B, Wen H J, Li Y H (2014). Sequence stratigraphy and paleogeography of the Middle Jurassic coal measures in the Yuqia Coalfield, northern Qaidam Basin, northwestern China. AAPG Bull, 98(12): 2531–2550

Li Y J, Li X J, Wang Y L, Yu Q C (2015). Effects of composition and pore structure on the reservoir gas capacity of Carboniferous shale from Qaidam Basin, China. Mar Pet Geol, 62: 44–57

Liang L X, Xiong J, Liu X J (2015). An investigation of the fractal characteristics of the Upper Ordovician Wufeng Formation shale using nitrogen adsorption analysis. J Nat Gas Sci Eng, 27(10): 402–409

Liu S X, Zhong J H, Ma Y S, Yin C M, Liu C L, Li Z X, Liu X, Li Y, Liu X G (2015a). Study of microscopic pore structure and adsorption isothermal of carboniferous shale, Eastern Qaidam Basin. Journal of China University of Petroleum, 39(1): 33–42 (in Chinese)

Liu X J, Xiong J, Liang L X (2015b). Investigation of pore structure and fractal characteristics of organic-rich Yanchang Formation shale in central China by nitrogen adsorption/desorption analysis. J Nat Gas Sci Eng, 22: 62–72

Loucks R G, Reed R M, Ruppel S C, Hammes U (2012). Spectrum of pore types and networks in mudrocks and a descriptive classification for matrix-related mudrock pores. AAPG Bull, 96(6): 1071–1098

Luo C, Liu S G, Sun W, Ran B, Wang S Y, Yang D, Bai Z Q, Ye Y C, Zhang X, Deng B (2014). Pore structure characterization of black shale in the Lower Cambrian Niutitang Formation in western Hubei and eastern Chongqing area. Journal of Northeast Petroleum University, 38(2): 8–17 (in Chinese)

Micromeritics Instrument Corporation (2012). TriStarII 3020 Operator's Manual. Georgia: C15–C20

Milliken K L, Rudnicki M, Awwiller D N, Zhang T (2013). Organic matter-hosted pore system, Marcellus Formation (Devonian), Pennsylvains. AAPG Bull, 97(2): 177–200

Montgomery S L, Jarvie D M, Bowker K A, Pollastro R M (2005). Mississippian Barnett shale, Fort Worth Basin, North-Central Texas: gas-shale play with multi-trillion cubic foot potential. AAPG Bull, 89 (2): 155–175

Nakagawa T, Komaki I, Sakawa M, Nishikawa K (2000). Small angle X-ray scattering sudy on change of fractal property of Witbank coal with heat treatment. Fuel, 79(11): 1341–1346

Pfeifer P, Avnir D (1983). Chemistry in noninteger dimensions between two and three. I. Fractal theory of heterogeneous surfaces. J Chem Phys, 79(7): 3558–3565

Pyun S I, Rhee C K (2004). An investigation of fractal characteristics of mesoporous carbon electrodes with various pore structures. Electrochim Acta, 49(24): 4171–4180

Qi H, Ma J, Wong P Z (2002). Adsorption isotherms of fractal surfaces. Colloid Surface A, 206(1−3): 401–407

Rigby S P (2005). Predicting surface diffusivities of molecules from equilibrium adsorption isotherms. Colloid Surface A, 262(1−3): 139–149

Shao L Y, Li M, Li Y H, Zhang Y P, Lu J, Zhang W L, Tian Z, Wen H J (2014). Geological characteristics and controlling factors of shale gas in the Jurassic of the northern Qaidam Basin. Earth Sci Front, 21(4): 311–322 (in Chinese)

Shao L Y, Liu L, Wen H J, Li Y H, Zhang W L, Li M (2016). Characteristics and influencing factors of nanopores in the Midddle Jurassic Shimengou shale in Well YQ-1 of the northern Qaidam Basin. Earth Sci Front, 23(1): 164–173 (in Chinese)

Sing K S W (1982). Reporting physisorption data for gas/solid systems with special reference to the determination of surface area and porosity. Pure Appl Chem, 54(11): 2201–2218

Tang X L, Jiang Z X, Li Z, Gao Z Y, Bai Y Q, Zhao S, Feng J (2015). The effect of the variation in material composition on the heterogeneous pore structure of high-maturity shale of the Silurian Longmaxi formation in the southeastern Sichuan Basin, China. J Nat Gas Sci Eng, 23: 464–473

Wang M, Xue H T, Tian S S, Wilkins R W T, Wang Z W (2015). Fractal characteristics of Upper Cretaceous lacustrine shale from the Songliao Basin, NE China. Mar Pet Geol, 67: 144–153

Wang X Z, Gao S L, Gao C (2014). Geological features of Mesozoic lacustrine shale gas in south of Ordos Basin, NW China. Petrol Explor Develop, 41(3): 326–337

Wu J G, Liu D M, Yao Y B (2014). Characteristics and controlling factors of nanopores in shales in Weibei, Ordos Basin. Oil & Gas Geology, 35(4): 542–550 (in Chinese)

Xiao Z H, Wang C H, Yang F R, Feng T, Wang Q R, Huang Y R, Chen X Y, Deng Y (2013). Reservoir conditions of shale gas in Lower Cambrian Niutitang Formation, northwestern Hunan. Acta Geol Sin, 87(10): 1612–1623 (in Chinese)

Xie H P (1996). A Study for Fractal and Rock Mechanics. Beijing: Science Publishing House, 93–95 (in Chinese)

Yang F, Ning Z F, Liu H Q (2014). Fractal characteristics of shales from a shale gas reservoir in the Sichuan Basin, China. Fuel, 115(1): 378–384

Yao Y B, Liu D M, Tang D Z, Tang S H, Huang W H (2008). Fractal characterization of adsorption-pores of coals from North China: an investigation on CH_4 adsorption capacity of coals. Int J Coal Geol, 73 (1): 27–42

Zhang D W, Li Y X, Zhang J C, Qiao D W, Jiang W L, Zhang J F (2012). The Evaluation of Shale Gas Resources and Potential Investigation in China. Beijing: Geology Publishing House, 70–78 (in Chinese)

Zhang J C, Jin Z J, Yuan M S (2004). Reservoir mechanism of shale gas

and its distribution. Natural Gas Industry, 24(7): 15–18 (in Chinese)
Zhu X M (2008). Sedimentary Petrology (4th ed). Beijing: Petroleum Industry Press, 208–286 (in Chinese)

AUTHOR BIOGRAPHIES

Haihai Hou is a post-doctoral scholar of geological resources and geological engineering in the College of Geosciences and Survey Engineering, China University of Mining and Technology, Beijing (CUMTB). He received his B.Sc. degree and M.Sc. degree from Henan Polytechnic University in 2009 and 2012, respectively. He obtained his Ph.D. degree from CUMTB in 2015. His research interests include sedimentology of coal-bearing measures and exploration of unconventional energy.

E-mail: houmensihai@163.com.

Longyi Shao is a professor at China University of Mining and Technology, Beijing, and serves as the vice Director of the College of Geosciences and Survey Engineering. He received his B.Sc. degree from Jiaozuo Mining Institute in 1983 and obtained his M.Sc. degree and Ph.D. degree from Beijing Graduate School of CUMTB in 1986 and 1989, respectively. He is currently leading an active group working on sedimentology and sequence stratigraphy of coal and oil basins in China.

E-mail: shaol@cumtb.edu.cn.

Yonghong Li is the geological director and a senior engineer at the Qinghai Bureau of Coal Geological Exploration. His major research interests are coal and associated minerals assessment and exploration.

E-mail: lyh6807@163.com.

Zhen Li is a M.Sc. candidate of mineral resource prospecting and exploration in the College of Geosciences and Survey Engineering, China University of Mining and Technology, Beijing. He received his B.Sc. degree from Henan Polytechnic University in 2014. His research interests are exploration and development of coalbed methane and shale gas.

E-mail: 1280436335@qq.com.

Wenlong Zhang is a deputy director at No.105 Exploration Team, Qinghai Bureau of Coal Geological Exploration. He received his B.Sc. degree from Shandong Agricultural University and obtained his M.Sc. degree from China University of Mining and Technology, Beijing. He has been engaged in coal geology and exploration, and basin analysis.

E-mail: 594088943@qq.com.

Huaijun Wen is a deputy director and senior engineer at the Qinghai Bureau of Coal Geological Exploration. He received his B.Sc. degree from Xi'an Mining Institute in 1987. His major research interests are coal geology and coal-bearing basin analysis.

E-mail: qh105whi@126.com.